DESIGN AND TESTING OF A HIGH-PRESSURE-RATIO CENTRIFUGAL STAGE – PROBING THE AERODYNAMIC & MECHANICAL LIMITS

James M. Sorokes
Principal Engineer,
Olean, NY USA

Kirk Lupkes
Engineering Manager, Seattle
Technology Center
Seattle, WA USA

Ravi Srinivasan, PhD
Lead CFD Engineer
Seattle, WA USA

Mark Kuzdzal
Director Business Development
Olean, NY USA

Dave J. Peer
Principal Development Engineer
Olean, NY USA

Silvano Saretto, PhD
System Technology Manager
Seattle, WA USA

All from the **Dresser-Rand** business
Part of Siemens Power & Gas

James M. "Jim" Sorokes is a Principal Engineer with the Dresser-Rand business with more than 40 years of experience in the turbomachinery industry. Jim joined Dresser-Clark (now the Dresser-Rand business) after graduating from St. Bonaventure University in 1976. He spent 28 years in the Aerodynamics Group, became the Supervisor of Aerodynamics in 1984 and was promoted to Manager of Aero/Thermo Design Enginering in 2001. While in the Aerodynamics Group, his primary responsibilities included the development, design, and analysis of all aerodynamic components of centrifugal compressors. In 2004, Jim was named Manager of Development Engineering whereupon he became involved in all aspects of new product development and product upgrades. In 2005, Jim was promoted to principal engineer responsible for various projects related to compressor development and testing. He is also heavily involved in mentoring and training in the field of aerodynamic design, analysis and testing.

Jim is a member of AIAA, ASME and the ASME Turbomachinery Committee. He has authored or co-authored more than 50 technical papers and has instructed seminars and tutorials at Texas A&M and the Dresser-Rand business. He currently holds four U.S. patents and has several other patents pending. He was elected an ASME Fellow in 2008. Jim was also selected as a Dresser-Rand Engineering Fellow in 2015.

Kirk Lupkes is the Engineering Manager responsible for technical and management oversight of the Dresser-Rand business' Seattle Technology Center team. He is a 1995 honors program graduate of Washington State University with a B.S. in Mechanical Engineering and a minor in Materials Science. He also received an M.S. in Mechanical Engineering from the University of Washington in 1997. He provided program management and technical oversight on the compressor development activities reported in this paper. He joined Dresser-Rand in 2014 and has worked in combustion and turbomachinery technology development for more than 20 years.

Mark J. Kuzdzal is the Director of Business Development for the Dresser-Rand business' supersonic compressor development initiative. In this role, Mark is responsible for product line management and business development to support supersonic compression technology. Prior to this assignment and for nearly a decade, Mark was the Manager of the Core Technologies organization for Dresser-Rand, where he oversaw Rotordynamics, Materials & Welding, Solid Mechanics, Aero/thermo dynamics and Acoustics disciplines.
Mark started his career with Dresser-Rand as a Rotordynamics engineer after earning a B.S. Degree (Mechanical Engineering, 1988) from the State University of New York at Buffalo. He has co-authored numerous technical papers and holds many U.S. Patents. Mr. Kuzdzal is an emeritus member of the Texas A&M turbo machinery advisory committee.

David J. Peer is a Principal Development Engineer with the Dresser-Rand business in Olean, New York. He has more than 40 years of experience in the application, design, and operation of centrifugal compressors. He was responsible for the design and development of single- and multi-stage pipeline compressor configurations. Among his accomplishments are the first Clark compressor with dry gas seals, the first Clark compressor with magnetic bearings, and the first centrifugal compressor to exceed 90% flange-to-flange efficiency. He is an inventor with multiple patents and has a BSME from the University at Buffalo in 1973.

Dr. Silvano Saretto is the System Technology Manager and the Aerodynamics team lead for the Seattle Technology Center (STC). Dr. Saretto is also the systems technical lead for the Pathfinder and Chamisa CAES programs. Prior to Dresser-Rand, he worked at Aerojet Corporation, Pratt & Whitney and was a Postdoctoral Scholar at the Pennsylvania State University. He has worked on combustion, turbomachinery, and advanced monopropellant rocket technology development for nearly 20 years. Dr. Saretto holds a Ph.D. in Energetics, a Laurea in Aeronautical Engineering from the Turin Polytechnic University, and a M.S. in Aerospace Engineering from the Pennsylvania State University.

Dr. Ravi Srinivasan is the Lead Aerodynamicist at the Seattle Technology Center (STC) and is responsible for CFD analysis related to projects executed at STC and high performance computing (HPC) activities related to Department of Energy (DOE) allocations and local systems. He has a B.E. (Bangalore University) and M.S. (The University of Alabama) in Mechanical Engineering and a Ph.D. in Aerospace Engineering from Texas A&M University. He has worked in high-speed flow phenomena, turbomachinery and gas turbine combustor analysis and internal combustion engines.

ABSTRACT

The paper describes the design, manufacture and testing of a novel high-pressure-ratio, single-stage centrifugal compressor targeted for use in high molecular weight applications. The stage was designed to deliver a minimum pressure ratio of 10:1 while also providing sufficient flow range to ensure stable operation, i.e., usable surge margin and overload capacity. The paper describes the motivation for the work, as well as the aerodynamic and mechanical design processes employed including a brief review of the analytical tools used. A high level overview of the aerodynamic optimization efforts is also presented.

The paper provides an overview of the test compressor, instrumentation, test loop and the data acquisition system, and addresses the "shake-down" testing performed with a baseline configuration to establish feasibility, ground the analytical predictions, and identify potential oversights in the design. Test results from an enhanced design developed via aerodynamic optimization are also discussed.

The paper closes with a review of the lessons learned and a summary of how the supersonic design extended the limits of what can be achieved with a centrifugal stage. Some thoughts regarding future work to enhance the performance of high-pressure-ratio stages and on the use of advanced optimization methodologies are also offered.

INTRODUCTION

As compressor original equipment manufacturers (OEM) have sought ways to provide more energy and space-efficient solutions for the oil and gas industry, attention has turned to the use of higher pressure ratio stages in process market centrifugal compressors. If more pressure or head rise can be attained in a reduced number of centrifugal compressor stages, the compressor case length can be decreased, allowing for more effective use of space on oil platforms, floating production storage and offloading vessels (FPSO), sub-sea systems, and the like. Further, if speed can be increased such that the pressure or head rise can be attained with lower diameter impellers, casing diameter can also be reduced.

High-pressure-ratio stages have been commonplace in turbochargers, gas generator sections of ground-based gas turbines, and helicopter engines for decades. Early gas turbine engines contained centrifugal compressor stages that achieved 3:1 pressure ratio or higher [McAnally, 1974, Rodgers, 1991, Japikse & Baines, 1994]. In the 1980s, the authors' company marketed a small gas turbine engine that contained a two-stage centrifugal compressor gas generator section, which achieved a pressure ratio in excess of 12:1. The authors' company also offers a gas turbine whose single-stage compressor reaches a pressure ratio of 7:1. Other turbocharger and helicopter engine OEMs have developed single-stage centrifugal stages that have achieved pressure ratios in excess of 13:1 in a single stage; however, virtually all of these stages operate on air at atmospheric inlet conditions and are only required to operate over a narrow flow range. High-pressure-ratio stages, by their nature, have a narrow flow range so they were acceptable for the applications mentioned.

Because oil and gas applications require wider flow ranges, high-pressure-ratio stages have historically been deemed a poor fit for such applications. However, the combination of movable geometry systems and optimized impeller and stationary component designs have helped partially overcome the range limit. This led to renewed interest in applying these stages in a broader range of centrifugal

machinery. In addition, as part of the Department of Energy's (DOE) Carbon Capture Program, the Dresser-Rand business has worked to develop higher-pressure-ratio stages specifically for carbon capture utilization and storage (CCUS) applications in which the CO_2 emitted by a fossil fuel-fired power plant is captured and compressed to pipeline delivery pressure. A unique aspect of this application is the ability to recover the waste heat generated by high-pressure-ratio stages and integrate the energy back into the power plant and capture system to decrease the overall energy penalty associated with the capture and compression system. This results in OPEX savings due to higher overall integrated system efficiencies, as well as CAPEX benefits associated with reducing the overall number of compressor stages required for a particular application.

It was this renewed interest in high-pressure-ratio compression applications that led the authors' company to pursue development of a supersonic, high power density turbomachine that could initially serve the CO_2 market for enhanced oil recovery (EOR) and carbon capture CCUS applications. Once developed, the technology would be expanded to work with any molecular weight gas. However, the initial focus was on higher mole weight gases because, as will be seen, there are many more challenges when designing compression systems for such gases. For example, when the compressed gas has a high molecular weight and when the inlet pressure is elevated, Mach numbers increase, temperature rise is higher, thrust loads are greater, etc.

As a secondary motivation, the authors were interested in determining how far high-pressure-ratio stages could be extended in both flow coefficient and in pressure ratio for higher mole weight applications. For example, it is commonly held that the optimum flow coefficient, ϕ, for best efficiency in conventional process compressor stages (i.e., Pr ≤ 2.0) is between 0.08 and 0.10. It is also well known that the peak attainable efficiency decreases as the pressure ratio increases. Further, high-pressure-ratio stages typically require higher impeller tip operating speeds; i.e., U2 > 1000fps (304m/s). These higher speeds lead to higher Mach numbers, which will limit the maximum flow coefficient for which viable high-pressure-ratio designs can be developed. Therefore, one would expect that the peak efficiency would occur at progressively lower flow coefficients as the target pressure ratio increased.

The paper describes the aerodynamic and mechanical challenges associated with the new design and discusses the steps taken to overcome those challenges. Also, given that the new design and operating requirements depart from the OEM's typical process compressor stage, a 2,200 PSIA (151.6 Bara) discharge pressure, 13,500 HP (10 MW) supersonic test facility and compressor were built to gather benchmarking and performance validation data.

A review of the test results to-date is provided, along with a summary of the lessons learned from the design and test efforts. Finally, a summary of future planned work is offered.

DESIGN CONSIDERATIONS

Before embarking on the new radial impeller stage design, the designers completed a literature survey to discern design guidelines or restrictions typically imposed for high-pressure stages. There are a large number of references available in the open literature and only a sampling are offered in the bibliography at the end of this paper. Discussions were also held with industry experts and consultants regarding known restrictions / limitations on high-pressure-ratio impellers and their associated stationary components, i.e., diffusers, volutes, etc.

The vast majority of the published literature focused on the impeller and diffuser design. Most included typical guidance regarding the need to minimize impeller inlet Mach numbers by controlling local curvatures in the meridional and blade profiles. All pointed to a need to minimize the running clearance on an open radial impeller configuration to achieve peak attainable efficiency. Most documents and experts also cited the need to avoid excessively tangential impeller exit flow angles so as to avoid premature impeller stall. In discussions with consultants and other industry experts, most suggested that the impeller exit absolute Mach number be kept below 1.2. This would prove to be a significant constraint in the aerodynamic design.

Since minimizing inlet Mach numbers is key to achieving an optimum design, a decision was made to pursue an overhung arrangement for the initial design. Such an arrangement allows a smaller impeller inlet shroud diameter because the compressor shaft need not pass through the impeller (See Figure 1). The lower shroud diameter, in turn, helps minimize the inlet relative Mach number. Knowing that the high-pressure-ratio and high Mach numbers would result in reduced choke and stall/surge margin, movable inlet guide vanes were implemented to provide a wider operating range. The pre-whirl would also impact the head rise capability of the impeller so the achievable pressure ratio would decrease as the amount of pre-whirl increased.

Another important discussion point was whether to use a shrouded or an unshrouded impeller. The vast majority of the high-pressure-ratio stages contain unshrouded impellers because the impellers need to run at high tip speeds, i.e., in excess of 2,000 fps (610 m/s), to achieve the necessary exit total pressure. Again, most of these applications were compressing air at atmospheric inlet conditions so the Mach numbers were not a major constraint. Given the gas properties of CO_2 as compared to air, one-dimension (1-D) calculations were sufficient to show that the tip speed would be restricted by the exit Mach number and that a high-pressure- ratio stage
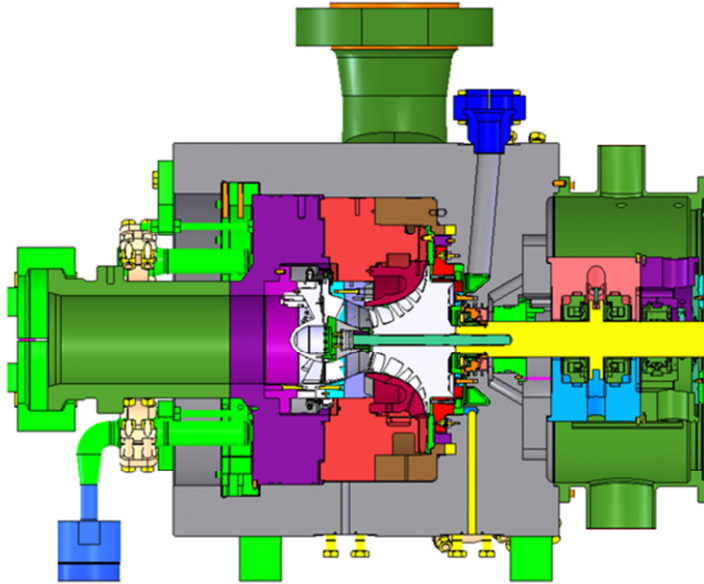
Figure 1 – Overhung impeller configuration.

compressing CO_2 had to run at a lower tip speed than one compressing air. These calculations also uncovered a potential roadblock to building a covered impeller: the temperature rise through the impeller from inlet to exit and the temperature gradient through the impeller cover itself with high temperature gas leaking down the outside of the shroud toward the impeller eye seal. The 1-D calculation estimated the temperature rise at 400°F (204°C), a significantly larger thermal gradient than experienced in most shrouded impellers. In response, stress analyses were conducted on the preliminary shrouded impeller geometries. These studies showed that the combination of the centrifugal and thermal stresses would exceed the allowable material limits between the impeller blades and a cover. Therefore, there was little choice but to proceed with an unshrouded impeller.

AERODYNAMIC DESIGN

The aerodynamic design followed a classic approach. Preliminary sizing was performed using 1-D bulk flow analyses using ConceptsNREC's Compal code. Though the performance models embedded in the code had not been tuned for the pressure ratios and Mach number required in this design, the preliminary numbers obtained were sufficiently accurate to provide adequate seed information for the remainder of the design process. These 1-D analyses uncovered several important considerations. First, to achieve a 10:1 overall static pressure ratio, the impeller must generate sufficient total pressure to ensure that the remaining static pressure rise could be achieved in the downstream radial diffuser and volute. Simply put, to achieve a flange-to-flange static pressure ratio of 10:1, the total pressure ratio across the impeller would have to be 13:1 or greater. The final impeller pressure ratio requirement would depend on the static pressure recovery attainable in the downstream stationary components. To ensure sufficient ratio in the impeller, it was assumed the stationary component would achieve 40% static pressure recovery. If this combined diffuser and volute static pressure recovery could not be met, the only choice was to further increase the impeller total pressure ratio.

The next issue uncovered during the 1-D scoping study was the impeller exit absolute Mach number, M_{2A}. The sonic velocity for carbon dioxide is 267 meters/second (m/s) at 1 atmosphere and 20°C, while the speed of sound in air under the same conditions is 344 m/s. This was a differentiator between the design being considered and the majority of the impellers described in the open literature (which compressed air). The high impeller exit velocity required to achieve the necessary exit dynamic pressure caused the exit absolute Mach number to exceed 1.3 for CO_2 compression. The same impeller exit velocities when compressing air would result in exit absolute Mach numbers lower than the 1.2 limit cited above. Therefore, a major focus during the impeller design process was investigating ways to reduce the exit absolute Mach number for the CO_2 applications.

The third consideration investigated in the 1-D study was the impeller exit flow angle. Again, the high tip speed required to generate sufficient total pressure at the impeller exit naturally led to a tangential impeller exit flow angle. If the angle became too tangential, rotating stall could occur immediately outside the impeller.

Keeping these design considerations in mind, a matrix of impeller geometries was generated across a range of total pressure ratios. Designs that provided the best combinations of aerodynamic characteristics were used to develop full three-dimension (3-D) geometries (i.e., hub, shroud and blade profiles). These 3-D geometries were next assessed using a streamline curvature analysis approach using ConceptsNREC's AxCent code. The two-dimensional (2-D) velocity profiles were used to fine-tune the meridional and blade geometries and to "weed out" poor designs prior to embarking on a full 3-D CFD simulation. Limited time was spent on this effort because the streamline curvature methodology would not properly capture the 3-D nature of the high Mach number impeller

flow field. However, the ability of such codes to converge in seconds allows designers to develop workable meridional profiles, thereby reducing the time spent on profile development with CFD simulations. That is, the 2-D code provides insight into the Mach number levels at the impeller inlet and exit so some adjustments were made in the impeller geometry to minimize these values. Further, it was also possible to do a preliminary assessment of splitter blade leading edge positions with the streamline curvature code.

As one might expect, computational fluid dynamics (CFD) played a vital role in the tuning of the impeller aerodynamic design. Analyses were conducted using the Numeca Fine/Turbo code and Ansys CFX. Typical CFD simulations were conducted using domain meshes containing 10Million-80Million grid points, depending on the simulated domain size and accuracy required. All the CFD simulations were conducted using the Spalart-Almaras turbulence model with wall function. For the higher fidelity simulations, grid size and wall clustering were selected to ensure an average y+ value of 1 or less. The low y+ value is to ensure that the CFD simulations provide accurate results for the near-wall effects, i.e., turbulence and boundary layer effects (Sorokes et al, 2016).

As the aerodynamic design of the impeller and diffuser often required satisfying conflicting design requirements, advanced optimization techniques were used in the design of the compressor. An overview of the optimization process is illustrated in Figure 2. Starting at the left in the figure, the image describes various steps accomplished during the process of optimization including: a) decisions on variable selection and range specification, b) using scripts and templates to generate geometry, grids and setup files for simulation execution, c) launching simulations on thousands of computer cores to evaluate the performance of all geometries, d) evaluation of responses for each geometry with respect to various input parameters, and e) generation of optimized samples and evaluation of responses. The process is repeated until the optimization converges. These processes are explained in more detail below.

The process of optimizing the compressor geometry begins with the generation of a parametric model of the flow path where 30-50 parameters are used to describe the entire impeller and diffuser flow path geometry. This initial parametrized geometry is then perturbed to generate a large database consisting of thousands of samples of derived geometries that are analyzed using CFD tools. The perturbed samples are selected to uniformly cover the design space. A key for successful aerodynamic flow path optimization is to select perturbation ranges for each parameter that are large enough to explore wide regions of the design space and yet restrictive enough to limit the number of nonsensical geometries generated in the process.

For each perturbed sample, several CFD simulations were conducted to determine their aerodynamic performance from choke to surge. The simulations were collected in large ensembles which were launched in parallel on the Oak Ridge Leadership Computation Facility (OLCF) Titan supercomputer.   Typically, the database generation required running tens of thousands of CFD simulations. Ensemble simulations were of such magnitude that in some cases they required utilization of 50-90% of the 290,000 cores available on the Titan supercomputer.

Post-processed information from these simulations was then analyzed using the software package, Minamo, and surrogate functions describing the response of key compressor design parameters, e.g., efficiency and range, were generated. Different sets of goals and constraints were specified to focus the optimization process in areas of interest in the design space. An iterative process was then used, which generated new geometry predictions via genetic optimization techniques to be evaluated using the same procedure as the initial database samples. Each iteration of the database analysis generated hundreds of additional geometries. Information from the original database, along with results from results of samples from optimization iterations, was re-analyzed at each intermediate step to refine the surrogate function accuracy and to predict a new series of optimized geometries. The optimization process was terminated when sufficient convergence had been reached. It was not possible to a priori foresee how many design iterations were required to reach convergence. In the high-dimensional setting, based on the team's experience with prior optimization projects, a typical minimum number was 10-20 design iterations, i.e. 10-20 updates of the database.

Data processing scripts were developed to automate the execution of a large number of simulations required for database generation. The inputs to these scripts were perturbed values of parameters of the geometry model and any associated simulation inputs, e.g. RPM. The scripts enabled generation of database geometry and grids in parallel using thousands of computer cores. Solution execution was accomplished in stages, given system and time constraints. A typical execution would be a launch of thousands of runs comprising of perturbed geometries at different operating points. Each simulation ran in parallel on hundreds of cores. Successful solutions were automatically identified and post-processing of these results was executed in parallel. Offline optimization and refinement of the database was performed, as outlined in the previous paragraph.

Due to the novelty of the impeller design and the potential for thermal and mechanical deformation of the impeller and adjacent components, a decision was made to obtain baseline test data on the impeller performance without the influence of the vaned diffuser. Data from this test would be used to calibrate or ground the CFD simulations. For example, does the impeller pass the flow rate and achieve the efficiency and pressure ratio predicted by the CFD analyses?
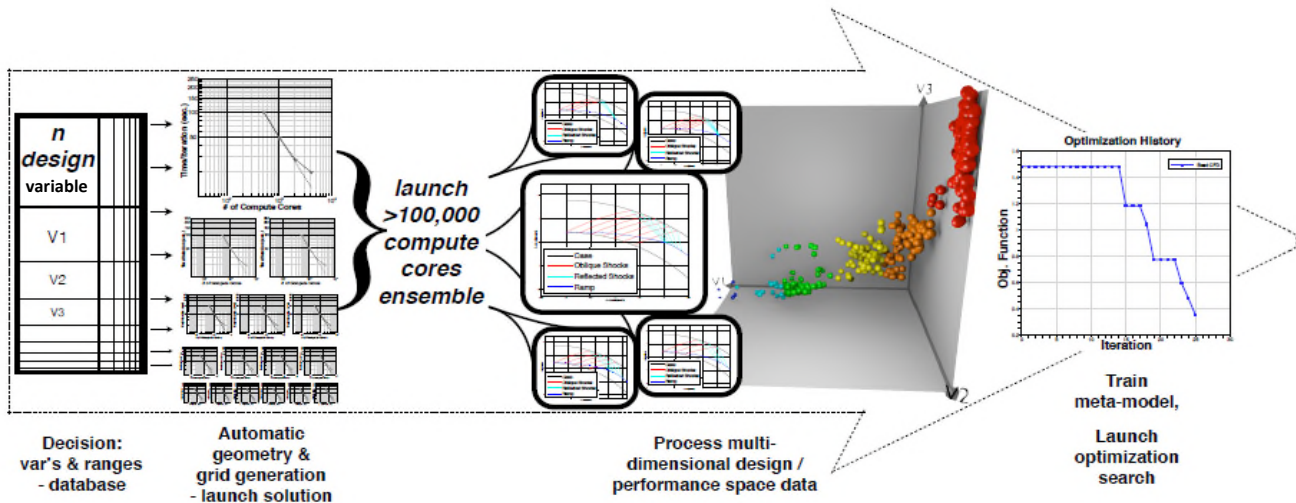
Figure 2 - Workflow of database ensemble computations, supporting design optimization.

WASTE HEAT RECOVERY

Early on in this program, it was recognized that doing more aerodynamic work in a smaller package resulted in a different path up the pressure versus enthalpy chart. As a result, a study was conducted to assess if the added compression power could be offset by harnessing mid-grade waste from the heat of compression. In traditional O&G applications, the compressor train is typically configured to minimize shaft power via gas intercooling and staying as close as possible to the isothermal compression line, the lowest power path up the pressure enthalpy chart. As shown in Figure 3, small pressure ratio steps with intercooling approach the near isothermal compression line. But, the heat of compression is not hot enough for efficient or economical waste heat recovery, so all the heat of compression is sent into the atmosphere.

The US Department of Energy National Energy Technology Laboratory (NETL) released a baseline study of power plants to investigate potential improvements. Case B12B described a supercritical pulverized-coal power plant with CO_2 capture where the CO_2 was separated from the amine solvent at 2 Bara, then compressed to 153 Bara for pipeline transport. The OEM evaluated the benefit of applying two stages of supersonic compression and recovering the heat of compression. In a typical CO_2 application with 80 °F (27 °C) gas entering the compression equipment, the gas discharge temperature exiting each stage is approximately 550 °F (288 °C). With gas intercooling between the two stages, two streams of approximately 550 °F (288 °C) gas is available for waste heat integration (see Figure 4).

The value of the recovered heat is dependent on where and how the heat is utilized. Co-optimization of the compressor train and boiler feed water heater (FWH) system enabled a substantial improvement in operating economics. A large fraction of heat of compression can be put to economic use, offsetting shaft power. In most instances with waste heat recovery, the supersonic compression solution will consume about 8-10% less net power when compared to a near isothermal compression solutions. As a side benefit the cooling water and cooling system load can be reduced by up to 80%.
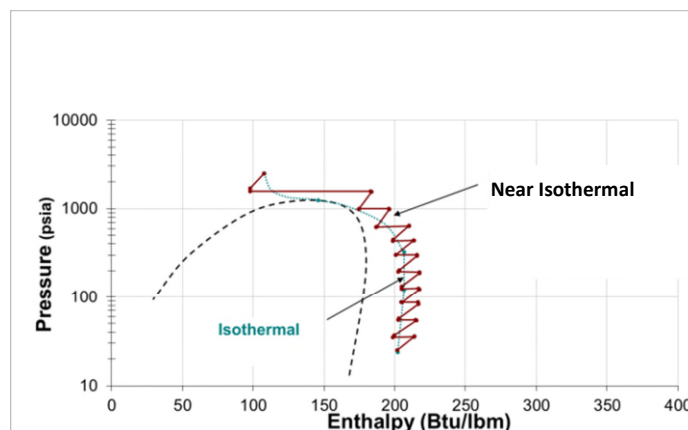

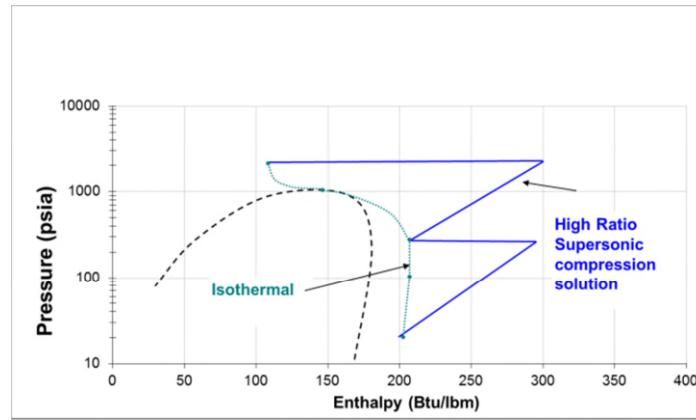**Figure 3. Pressure versus Enthalpy for near isothermal compression.**

Figure 4. Pressure versus Enthalpy for high-ratio compression.

MECHANICAL DESIGN

As shown in Figure 1, the compressor features a relatively conventional, single-stage, overhung configuration with a tie-bolt shaft assembly. The impeller is mounted to the shaft with a Hirth-type connection to facilitate torque transmission at high speeds and enable centering the impeller to the shaft. Given the unshrouded design of the impeller, it was also important to control the centering of the static bundle and shroud components to achieve good alignment to the impeller with minimum blade tip clearance.
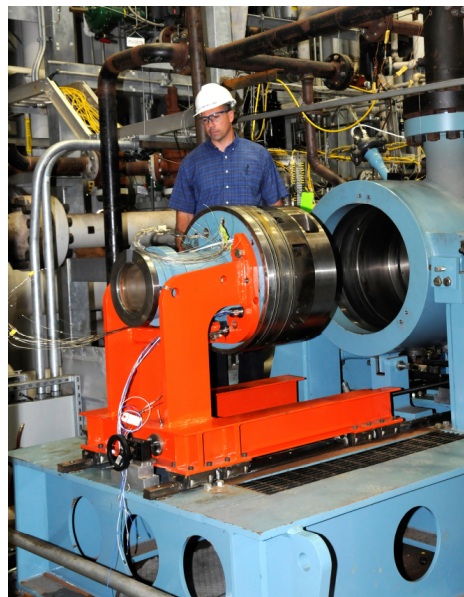

Figure 5. Compressor bundle installation into pressure case.

The mechanical design presented a number of unique challenges, most of which directly resulted from the high operating speeds and temperatures generated by a 10:1 pressure ratio compressor suitable for long-term industrial applications. These challenges required coupled thermal-structural analysis and iterations with the aerodynamic design to achieve a unit that simultaneously met rotordynamic, structural and life requirements, while meeting overall compressor performance goals.

The combination of high speed (greater than 30,000 RPM in some tests) and high power (10 MW) required the use of a 3,600 RPM motor with a compound epicyclic gear with a ratio approaching 10:1. Ultimately, the drivetrain achieved reliable operation with minimal drivetrain parasitic loss due to the relatively low oil flow rates required by the epicyclical gear relative to more conventional parallel gear sets.

Although the focus of this testing program was to validate aerodynamic predicted performance, from a mechanical perspective this compressor redefined the boundaries of centrifugal compressor experience in many areas. The 10:1 pressure ratio on CO_2 is certainly a new frontier. The stage delta-p is about twice as high as those found in a typical reinjection compressor. High speed and high delta-p demand naturally conflicting counter-measures. On one hand you have centrifugal stresses dictating reduction of thickness

7

and on the other hand you have pressure-related structural loads calling for more robust sections. Adding to the challenges, the high-pressure-ratio is accompanied by high-temperature-ratio. Again, it is not so much the ratio as the discharge temperature and the gradient across the stage. Thermal stresses are caused by gradients and yield strengths are limited by temperature.

As always, rotor dynamics were an important consideration during the design process and the new compressor was not without its challenges to that discipline. As mentioned earlier, the aerodynamic design of the stage is based on an established single-stage overhung rotor configuration, chosen to minimize the impeller inlet relative Mach number by minimizing the shroud diameter at the blade leading edge. As a result, the supersonic impeller has a relatively small hub diameter driving the design to utilize a Hirth coupling and a tie bolt to carry the torque and power (see Figure 6).
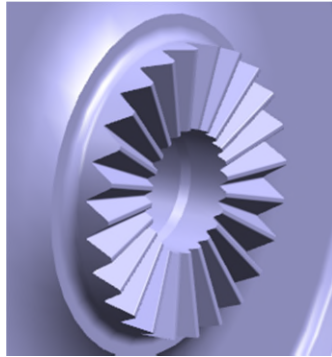

Figure 6. Shaft to impeller power transmission path.

The Hirth, or Vee-tooth interface was chosen because the feature could be positioned away from the highest stress area and would not only transmit the torque but also would allow radial growth of the impeller while maintaining concentricity. Also, it is fairly easily machined by a large number of sources and does not require proprietary cutter tooling. Manufacturing of this interface was given special attention to ensure that the tolerances for alignment and concentricity of the assembled rotor were achieved. A central tie-bolt secures the impeller tightly to the shaft, regardless of the speed or torque.

While a cantilevered rotor configuration might be optimum for meeting the aerodynamic objectives, the rotor dynamics are more difficult for a number of basic reasons.

For the same distance from the impeller to the bearing, the displacement of a cantilevered impeller as a result of shaft bending is greater than for an impeller on a beam style rotor. The stiffness of the overhung shaft, i.e., length and diameter, has to be engineered such that it is high enough for the bearings to be effective.

Critical Speeds and Unbalance Response: Control of the response frequencies and separation margins followed a conventional approach of selecting suitable shaft diameters to produce the necessary stiffness. The first step is to make the overhang as short as possible and then increase the shaft diameter as necessary. After a few iterations, the bearing and seal diameters of a similar, but slightly larger, legacy rotor are found to satisfy the requirement of both stiffness and torsional stress.

Bearing Design: Because the impeller must rotate at a high tip speed to generate the necessary exit dynamic pressure needed to achieve the 10:1 stage pressure ratio, the bearing surface speeds are higher than in typical turbo compressors. The commonly held maximum surface speed for a conventionally lubricated hydrodynamic journal bearing is 250 fps (76 m/s). For higher speeds, the use of directed lubrication and an oil-evacuated housing are required. Even so, most commercial experience ends at 300 fps (91m/s). The journal bearing surface speed for this rotor is 412 fps (126 m/s). The situation for the thrust bearing paralleled that of the journal bearings.

The design used tilt pad journal and thrust bearings. The heat generated within the bearing is roughly related to the square of the surface speed. This heat is carried away by the bearing lubricant and dictates the bearing oil flow rate. The as-tested bearing pad temperatures are shown in Table 1. The design complied with API-617 7th edition, which requires pad temperatures to be below 212 °F (100 °C) at the design conditions.

Table 1. Test bearing pad temperatures

Bearing	Speed (RPM)	Load (PSI)	Measured Pad Temperatures (°F)
Thrust	27635	283	187.0
Impeller End Journal	27635	15	188.0
Coupling End Journal	27635	5	182.0

Stability: Rotordynamic stability is evaluated by calculating the damping associated with the rotor natural frequencies, primarily the first forward mode. The classic stability measure, logarithmic decrement, is the rate of decay of vibration when the rotor is exposed to an excitation. A negative number indicates the vibration grows and the system is unstable. In addition to modeling the rotor and bearings, the stability analysis includes the destabilizing aerodynamic effects of internal stage hardware to determine how the rotor will behave while performing its intended function [Gupta, Wachel]. Aerodynamic cross-coupling is modeled as a destabilizing stiffness, meaning that a displacement of the rotor causes a proportional non-restoring force. API-617 provides a formula for calculating the cross-coupling effect:

$$q_a = \frac{3 \times (HP) \times 63}{D_c \times H_c \times N_r} \left(\frac{\rho_d}{\rho_s}\right) \, lb/in$$

Where:
HP is horsepower
H_c is tip width, inches
D_c is tip diameter, inches
N_r is speed, rpm
ρ is density at suction and discharge

The density ratio for this stage is high and the tip width is relatively small, resulting in large predicted values of cross-coupling. The predicted cross-coupling for an impeller operating on CO_2 at a 10:1 pressure ratio is more than 20 times greater than for the same stage running on air at 1,000 fps (305 m/s).
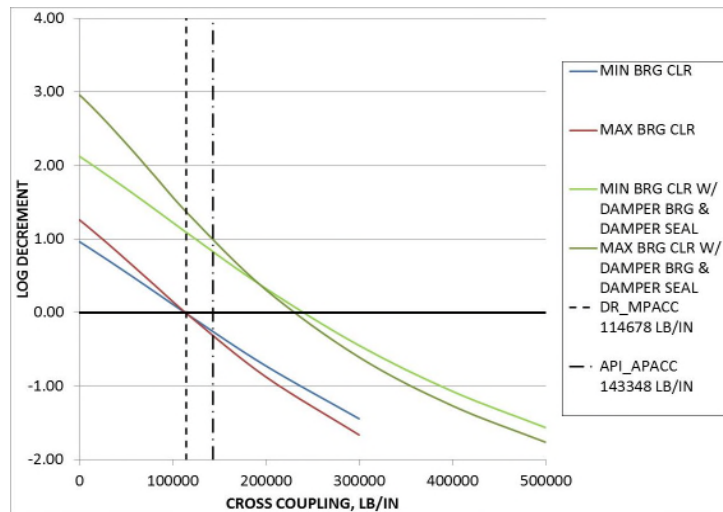
CURVE	BRG CLR	ANALYSIS LEVEL	AERO CROSS COUPLING LB/IN	LOG DEC	STABILITY THRESHOLD LB/IN	THRESHOLD RATIO
1	MIN	1	143348	-0.257	113448	0.79
2	MAX			-0.314	114273	0.80
3	MIN	2	114678	1.091	242452	2.11
4	MAX			1.369	234024	2.04

Figure 7. Passive excitation plot.

The results of the stability analysis are shown in Figure 7. The rotor stability (log dec) is plotted for maximum and minimum bearing clearances over a range of applied cross-coupling. Log dec is the logarithm of the ratio of the system amplitude on successive cycles of vibration. A positive number indicates the vibration amplitude is decaying with time. A negative number indicates that the vibration is growing, i.e. unstable. Cross coupled stiffness is applied to the impeller in increasing quantities. As the aerodynamic cross-coupling increases, the stability decreases and eventually the rotor is analytically predicted to go unstable. The vertical lines represent the expected values for cross coupling. The value using the API formula is 143,348 lb./in. There is some uncertainty concerning application of the API formula as these stage design conditions are well outside of the experience.

The Level 1 stability analysis was completed with a squeeze film damper added to the lightly loaded coupling end bearing. The stability threshold was predicted to be 114,000 lb./in.; insufficient to pass a Level 1 analysis. Because the rotor was predicted to be unstable, a level 2 analysis, which includes stiffness and damping from seals, was required by API. Seals were added to the analysis model and a new estimation of the impeller cross-coupling value was used. A hole-pattern damper seal was designed for use at the

balance piston location. In this more detailed Level 2 analysis, the rotor was deemed to be stable and met both internal and API acceptance criteria. The stability threshold had increased to 234,000 lb./in. The vertical lines represent the expected values for cross-coupling. The value using the API formula was 143,348 lb./in. The stability ratio is the predicted threshold of instability divided by the expected cross coupling, or 1.63 for this level 2 analysis.

Damper Seal Design: The results of the stability analysis dictated that the hole pattern seal must function properly through the entire period of operation, from the time the rotor first comes up to speed, through the transient conditions, and on to steady-state operation. The design of the shaft attachment required the impeller thrust to be inherently balanced. Consequently, the balance piston was made integral with the impeller and could not be thermally or structurally isolated from it. The seal characteristics are dependent on the dimensions of the clearance gap across the width of the seal. The deformed contour of the seal bore and the deflected shape of the impeller had to be designed to complement each other. It is necessary to avoid a situation where distortion of the interacting surfaces could result in a leakage path that produces a negative effect on the rotor.

The unit was tested at full load and full pressure and demonstrated no sub-synchronous vibration, validating the rotor dynamics stability analysis (see Figure 8). Vibration spectra for the impeller end and coupling end vertical probes are shown. The compressor operating speed is highlighted. The 340 Hz component corresponds to a diffuser pressure pulsation and is not a rotor natural frequency.
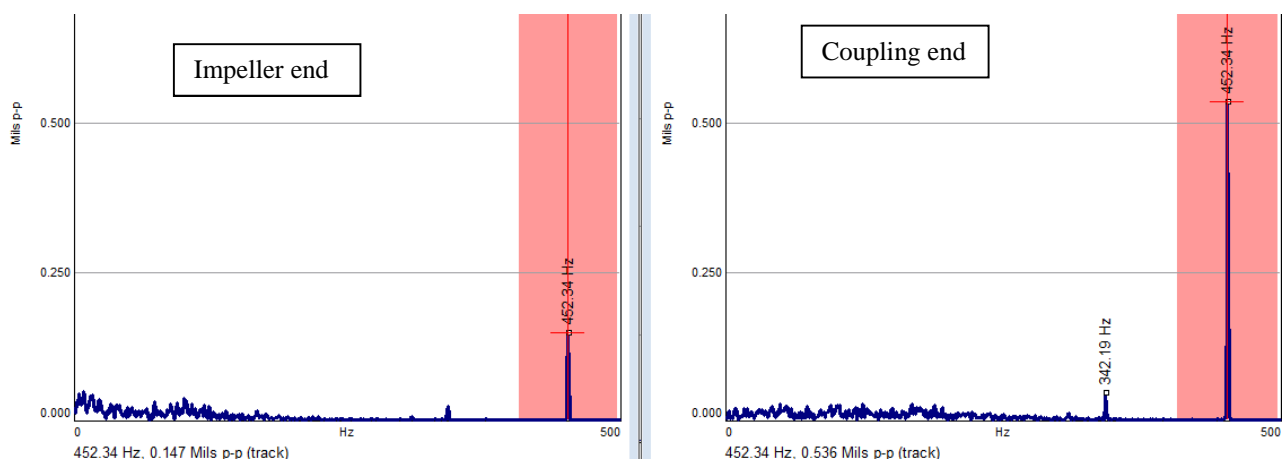

Figure 8. FFT showing no subsynchronous vibrations.

Mechanical Design & Impeller Blade Tip Clearance: The initial assumption for the impeller mechanical design was that it would be a shrouded or covered design; however, early in the design process (as discussed earlier in this paper) it became apparent that this would not be possible. The tip speeds of this aerodynamic design necessitated a move to a titanium alloy with adequate specific strength. Moving to an open impeller design requires maintaining rotor-stator clearances suitable to achieve the required aerodynamic behavior and performance.

Both low-cycle and high-cycle fatigue conditions were analyzed. A dynamic impeller audit (Schiffer, 2006) was conducted to ensure that interaction of the impeller with the inlet guide vane (IGV) and diffuser vanes would not cause a resonant condition. Nonlinear harmonic CFDs were run to evaluate the structural load on the impeller when the movable inlet guide vanes (MIGVs) were rotated.

The tip gap requirements at design point were achieved by considering the relative movement of the impeller and stationary shroud through the operating cycle. By appropriate material selection and geometric profiling of the shroud and a hot-to-cold conversion of the impeller using aerodynamic, inertial and thermal loads, it was possible to achieve the required impeller blade tip gap. In order to mitigate the effect of any unforeseen rubs, an abradable coating was applied to the shroud in conjunction with a suitable hard coating of the impeller blade tips. The shroud clearance has an impact on performance. To assure that the running clearance was known explicitly throughout the course of testing, a tip gap measurement system was developed and monitored continuously.

Impeller operating temperatures were computed through a conjugate CFD thermal analysis to properly account for heat transfer from the balance piston cavity to the flow path. The hottest spot is the result of fluid shear in the seal area and is also influenced by the seal leakage rate. The magnitude of the temperature rise varied with the speed, pressure differential and clearance. The results were supported by test data.

The gas discharge temperature increases simultaneously with the speed. The impeller, exposed to high convection coefficients, follows with very little lag time. Managing the seal clearance during this transient period was the focus of a great deal of analysis. A large clearance is the simplest solution to prevent the hot impeller from touching the seal while it's still cool. The downside is reduced

damping and high leakage during normal operation. In the end, mechanisms were added to increase the thermal response of the seal and reduce the impeller temperature. As part of the test, high temperature radial position probes were embedded into the seal ring to continuously monitor the clearance.

Compressor Design for High Temperature: Operating rotating equipment in an environment exceeding 500 °F (260 °C) is not unusual. Operation above 2,000 psig and 500 °F (260 °C) is less common. Shortening the overhang for rotordynamic reasons resulted in close proximity of the dry gas seal and high temperature leakage from the damper seal. The operational limit of the dry gas seal is 380 °F (193 °C) so a number of features were developed to isolate the seal.

As shown in Figure 1, just upstream of the impeller are moveable vanes to guide the flow into the stage. These were deployed to increase the flow range of the stage. Three discrete vane setting angles are shown in Figure 9. "Co-swirl" refers to the guide vanes turning the flow in the same direction as the rotor is turning and "counter swirl" turns the flow against rotor rotation. Later in this paper, the predicted and measured flow shift as a result of actuating the moveable inlet guide vanes are shown in Figure 13 and Figure 14.
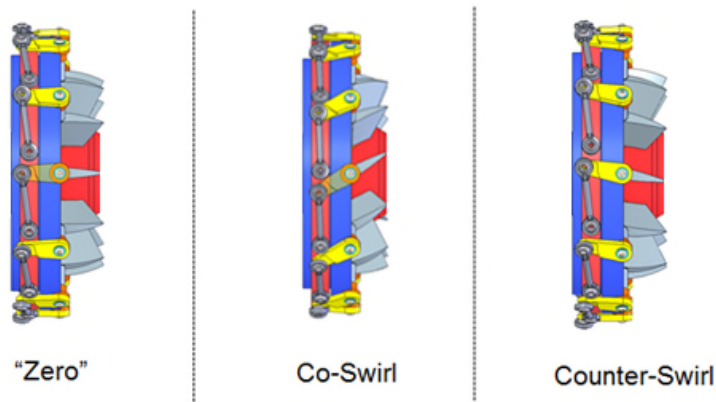

Figure 9. Actuation of Movable Inlet Guide Vanes

TEST FACILITY

A dedicated high-pressure (up to 2,350 psig discharge) (162 bar) CO_2 test facility was built on the OEM's campus to support full-scale development testing of high-pressure-ratio compressor stages. See Figure 10 for an external view of the main test building (foreground right) and dedicated control room (foreground left). An internal view of the main test building with a single-stage compressor installed on the test stand is given in Figure 11.

Figure 10. High-pressure CO_2 compressor test facility.

Figure 11. CO$_2$ compressor on test stand.

TEST PROGRAM

The initial target application for the supersonic compressor was CO$_2$ reinjection for EOR or carbon capture (CCUS). These systems operate at high pressure with many having discharge pressures exceeding 2,200psia (151 bara). Therefore, it would not be possible to validate the new stages using the low-pressure test rigs typically used for performance verification. A new, high-pressure casing was developed following guidelines used for the OEM's successful radially-split compressors. A special head was developed to accommodate the axial inlet, and the discharge volute and nozzle were based on the OEM's sub-sonic centrifugal product line.

Given the high-pressure-ratios and high Mach numbers involved, the amount and types of instrumentation installed in the compressor section were selected with great care. There was standard instrumentation (i.e., total pressure, static pressure, total temperature probes) in the inlet and discharge spool pieces. These were used to assess the overall compressor performance. In addition, there were static pressure taps at key locations in the internal flow path; i.e., at the impeller inlet, along the impeller shroud surface, at the impeller exit, and at three locations in the diffuser. Total pressures were also measured at the impeller inlet and dynamic pressure probes were installed in the diffuser to detect any pressure pulsations that might occur due to rotating stall or other aero-mechanical phenomena. The instrumentation locations and number of probes are shown in Figure 12.
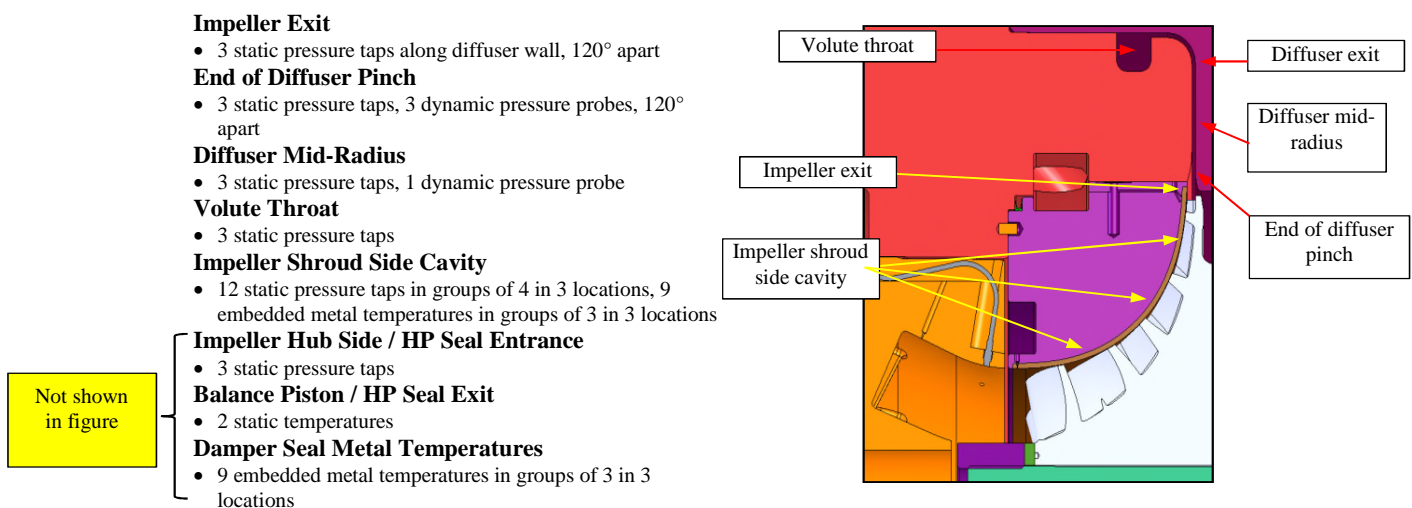
Impeller Exit
- 3 static pressure taps along diffuser wall, 120° apart

End of Diffuser Pinch
- 3 static pressure taps, 3 dynamic pressure probes, 120° apart

Diffuser Mid-Radius
- 3 static pressure taps, 1 dynamic pressure probe

Volute Throat
- 3 static pressure taps

Impeller Shroud Side Cavity
- 12 static pressure taps in groups of 4 in 3 locations, 9 embedded metal temperatures in groups of 3 in 3 locations

Impeller Hub Side / HP Seal Entrance
- 3 static pressure taps

Balance Piston / HP Seal Exit
- 2 static temperatures

Damper Seal Metal Temperatures
- 9 embedded metal temperatures in groups of 3 in 3 locations

Not shown in figure

Figure 12. Schematic showing instrumentation location

There were also proximity (capacitance) probes installed in the stationary impeller shroud to monitor the impeller blade running clearance during operation. These proved to be very valuable because, as noted above, the performance of the unshrouded impellers is dependent on minimizing the tip gap between the blade tips and the adjacent shroud.

TEST RESULTS

Several tests have been completed to date. As noted earlier, initial "shake-down / baseline" runs were completed on the first generation impeller with a vaneless diffuser to characterize the aerodynamic and mechanical behavior of the impeller and rotor system. These runs provided a calibration baseline between the analytical and test results but also uncovered opportunities to further improve the mechanical aspects of the unit. As expected, this initial configuration fell short of the 10:1 pressure ratio goal. It also fell short of the performance levels from the CFD simulations. Data showed that the impeller was providing the necessary exit velocity pressure, but at design speed, the stage attained a pressure ratio of 8:1 and the stage efficiency was below the target. The pressure recovery in the vaneless diffuser was lower than predicted by CFD. Given the shortfall in performance, the focus of the remainder of this initial testing series turned to studying the rotor dynamic and mechanical aspects of the overhung configuration with the open impeller.

One other noteworthy aero-mechanical attribute was the non-uniform pressure field induced in the vaneless diffuser by the discharge volute. It is commonly known that a volute will cause a non-uniform pressure distribution upstream of the volute due to the volute tongue or "cut-water" (Borer et all, 1997, Sorokes et al, 1998). In most compressors, the non-uniformity is small, with little impact on the stage aerodynamic performance and of little consequence mechanically as the forces can be easily accommodated by the radial bearings. However, in this initial vaneless diffuser test, the non-uniformity was larger than expected, causing diffuser losses that contributed to low stage efficiency. The resulting radial forced also led to high bearing forces. Though a problem during the "shake-down" testing, this volute-induced non-uniformity was not expected to be a problem in future tests because the vaned diffusers planned for subsequent builds would effectively isolate the rotor from the non-uniform pressure field of the volute (Sorokes & Koch, 2000).

Testing began on the second generation impeller and vaned diffuser in 2015. The new stage performance was closer to the efficiency target but further improvement was required. The pressure ratio was slightly short of the 10:1 target at the design speed, achieving a pressure ratio of 9.3:1. The flow range was close to predicted. Testing was also completed over the full range of the MIGV. As expected, the pressure ratio dropped as the MIGV added positive pre-whirl or co-swirl into the impeller. Due to the high inlet relative Mach numbers, negative pre-whirl or counter-swirl did not result in a noteworthy increase in the pressure ratio.

In an effort to exercise the capabilities of the stage, a decision was made to increase the speed to the maximum allowable based on the impeller stress analysis. During a test in November 2015, the operating speed was increased by 1.5% and the stage achieved the 10:1 target static-to-static pressure ratio. During testing in December 2015, the speed was increased to the maximum attainable operating speed and the compressor achieved a pressure ratio of 11.5:1. As expected, at this higher pressure ratio, a reduction in both efficiency and overall operating range as seen in Figure 12. However, even at this high pressure ratio, the stage still provided usable operating range.
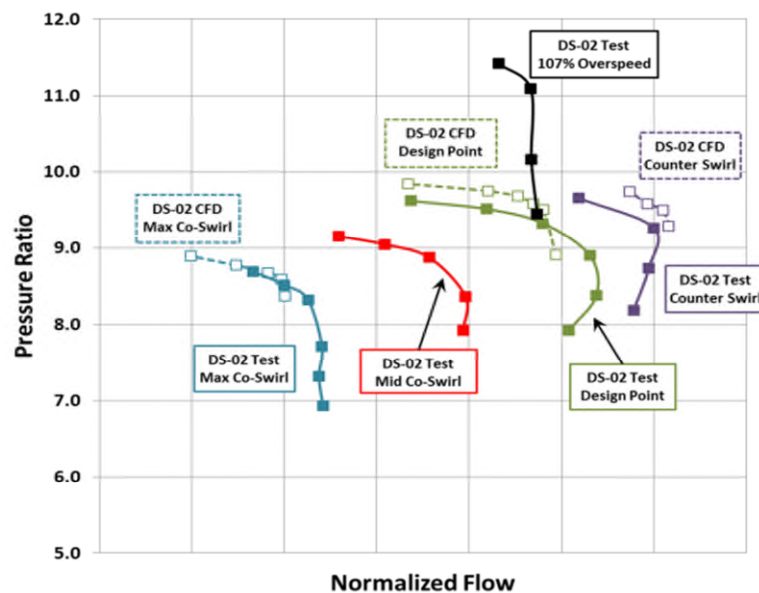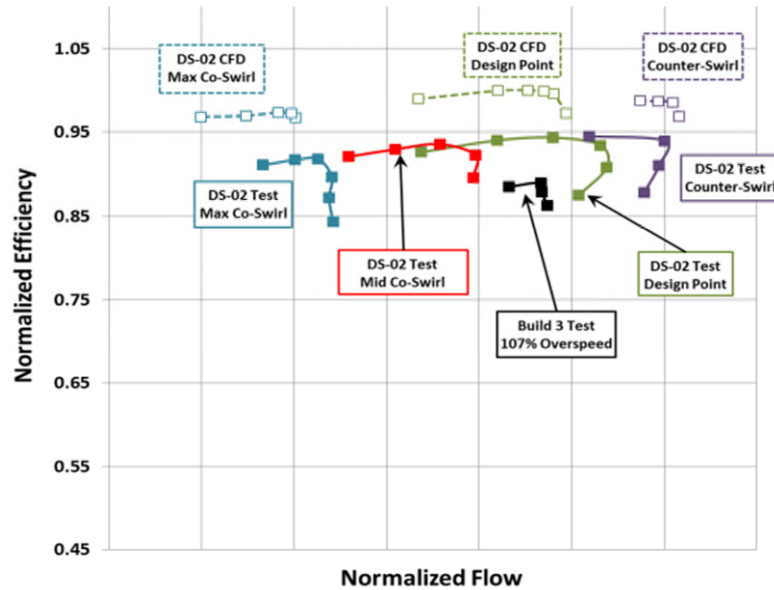

Figure 13. Stage pressure ratio.

Copyright© 2017 by Turbomachinery Laboratory, Texas A&M Engineering Experiment Station

Figure 14. Stage normalized efficiency.

LESSONS LEARNED

Several very valuable lessons were learned or re-enforced during this effort and are listed below:

- First, it is very important to include the entire flow path, including secondary flow passages, in the CFD simulations when assessing the overall performance and the aero-mechanical forces associated with high-pressure-ratio, high mole weight applications. It is equally important to consider the thermal effects resulting from the high temperature rise that can occur in such applications. The latter had a significant impact on the mechanical design of the primary flow path components (i.e., the impeller and diffuser) as well as the secondary flow path components (i.e., the balance piston, balance piston seal, gas seals, etc.).
- Second, the CFD simulations and test results reinforced the critical importance of the impeller running clearance in achieving high efficiency and pressure ratio. Further, if the running clearance was not kept low enough, it became more difficult to control the flow rate in the test vehicle.
- Third, the improvement obtained between the first and second iteration of the impeller confirmed the value of the optimization methods, i.e., Minamo and the surrogate functions. Allowing the optimizer to search for improved configurations reduced the amount of engineering time typically spent on manual manipulation of the geometry.
- Fourth, several long-held mechanical design limits related to stage pressure rise, bearing surface speeds, and the like were successfully exceeded, leading to a need to re-write the rule book.
- Fifth, similar long-held aerodynamic design guidelines were also violated. One of note was the belief that it is not possible to achieve stable aerodynamic operation with an impeller exit absolute Mach number in excess of 1.3. Testing on this compressor proved otherwise.
- Finally, this testing provided valuable insight into the achievable pressure ratios for heavier molecular weight gases. While pressure ratios in excess of 10:1 have been achieved for air and lighter molecular weight gases, the increased Mach numbers associated with CO_2 and heavier gases become the limiting factor. At the lighter molecular weights, impeller stress levels and/or tip speeds tend to be the limiting factors; though ultimately Mach numbers will limit the achievable pressure ratio at lower molecular weights as well.

FUTURE WORK

Given the success achieved via the optimization effort on the second generation impeller, a decision was made to conduct further optimization efforts on the vaned diffuser. There are also questions regarding how far the high-pressure-ratio concept can be extended to higher flow coefficient impellers. It is not expected that the concept can be extended to the full range of flow coefficients typically applied in process market compressors. Given the high tip speeds required to generate the necessary impeller exit kinetic energy, the inlet relative and exit absolute Mach numbers will certainly limit the maximum flow coefficient. Studies will be completed to determine this limit. Further tests will be conducted to confirm the achievable efficiency and to validate the CFD simulations completed for the higher flow coefficients.

CONCLUDING REMARKS

The paper provided an overview of a research and development program whose primary goal was to develop a high-pressure-ratio, single-stage compressor design for CO_2 applications. The program's secondary goal was to probe and possibly extend the aerodynamic and mechanical limits for such designs, with the ultimate objective being to offer novel or ground-breaking solutions to the process compressor market.

Above all, the project provided significant insight into the issues associated with extending the high-pressure-ratio concept, such as:
- Increased Mach numbers and their impact on stage and component performance;
- Pressure non-uniformities induced by the volute;
- Thermal loads or forces due to the increased temperature rise across the impellers;
- Control of impeller tip gap leakage at the higher operating speeds, pressures, and temperatures;
- Challenges associated with obtaining accurate CFD simulations given the complexities of the geometry and gas conditions.

The test and analytical experiences have helped establish enhanced design guidelines and assessment criteria that can be applied in the development of higher pressure ratio stages for the process industry. Further, by probing the limits via the 10:1 pressure ratio on CO_2, future designs targeting lower pressure ratios and/or lower molecular weights are now interpolations of existing technology rather than extrapolations. The program established the upper bound (or at least the near upper bound) of the high-pressure-ratio concept so that the effort and challenges associated with new designs between the current conventional process stage and the upper bound are known.

This work also challenged the capability of conventional aerodynamic and mechanical analytical tools and modeling techniques. This effort required the use of more advanced methods and more comprehensive computational models not typically used by the process compressor industry, i.e., optimization systems, models that included secondary flow paths. Methods such as modeling fluid-structure interactions, non-linear harmonic (NLH) simulations in CFD, conjugate heat transfer analyses, adaptive optimization system and the like must become part of the design process to be successful with these novel designs. The experiences helped the OEM establish a more robust, advanced design/analysis system that will be needed for future compressor development.

In closing, the application of high-pressure-ratio stages is an attractive alternative when developing compact, high-energy-density compression systems. The program described in this paper represents a significant step forward in understanding the technologies required and the aerodynamic and mechanical limits that must be faced when designing such stages.

REFERENCES

Borer, C.J., Sorokes, J.M., McMahon, T., and Abraham, E.A., "An Assessment of the Forces Acting Upon a Centrifugal Impeller Using Full Load, Full Pressure Hydrocarbon Testing," Turbomachinery Symposium Proceedings, Texas A&M, 1997.

Came, P.M., Robinson, C.J., "Centrifugal Compressor Design," Developments in Turbomachinery Design, pp135-151, 1999.

Gupta, M. and Childs, D., "Rotordynamic Stability Predictions for Centrifugal Compressors Using a Bulk-Flow Model to Predict Impeller Shroud Force and Moment Coefficients," Proceedings of ASME Turbo Expo 2006, Power for Land, Sea, and Air; May 8-11, 2007, Montreal, Canada, 2006.

Japkise, D., Baines, N., Introduction to Turbomachinery, Concepts ETI, Inc. and Oxford University Press, 1994.

McAnally, W.J. III, "10:1 Pressure Ratio Single Stage Centrifugal Compressor Program," U.S. Army Air Mobility Research & Development Laboratory, West Palm Beach FL, 1974.

Rodgers, C., "The Efficiencies of Single-Stage Centrifugal Compressors for Aircraft Applications," ASME paper 91-GT-77, 1991.

Rusch, D., Casey, M., "The Design Space Boundaries for High Flow Capacity Centrifugal Compressors," ASME paper GT2012-68105, 2012.

Schiffer, D. and Syed, A., An Impeller Dynamic Risk Assessment Toolkit, 35th Texas A&M Turbomachinery Symposium, Pages 49-54, Texas A&M, 2006.

Senoo, Y., Ishida, M., "Deterioration of Compressor Performance Due to Tip Clearance of Centrifugal Impellers," Journal of Turbomachinery, pp 55-61, 1987.

Sorokes, J.M., Borer, C.J., and Koch, J.M., "Investigation of the Circumferential Static Pressure Non-Uniformity Caused by a Centrifugal Compressor Discharge Volute," ASME paper no. 98-GT-326, 1998.

Sorokes, J.M. and Koch, J.M., "The Influence of Low Solidity Vaned Diffusers on the Static Pressure Non-Uniformity Caused by a Centrifugal Compressor Discharge Volute," ASME paper no. 00-GT-454, 2000.

Sorokes, J., Hardin, J., Hutchinson, B., "A CFD Primer: What Do All Those Colors Really Mean?" Turbomachinery Symposium Proceedings, Texas A&M, 2016.

Wachel, J. C., and von Nimitz, W. W., "Ensuring the Reliability of Offshore Gas Compressor Systems," Society of Petroleum Engineers of AIME, Journal of Petroleum Technology, Nov., pp.2252-2260, 8, 1981.

NOMENCLATURE

Dc = Impeller tip diameter, inches
Hc = Impeller tip width, inches
HP = Horsepower
M_{2A} = Impeller exit absolute Mach number
Nr = Rotor speed, rpm
ρ = Density at suction and discharge
U2 = Impeller tip speed (feet per second)

ACKNOWLEDGEMENTS